

Application Note

Calibration of AMR Angle Sensors



Scott Bryson

ABSTRACT

Anisotropic magneto-resistive (AMR) sensors are magnetic sensors that detect the direction of the magnetic field vector rather than the strength of the field. An AMR sensor determines the position of a rotating permanent magnet if the field is sufficiently strong. AMR sensors can typically only resolve up to 180°.

[TMAG6180-Q1](#) and [TMAG6181-Q1](#) both implement AMR sensing combined with a 2D Hall-effect latch to expand angle calculations to a full 360° for low-latency angle measurements. TMAG6180-Q1 produces outputs Q0 and Q1 which provides quadrature data for absolute angle measurements and TMAG6181-Q1 includes a turns counter function which tracks relative position even while operating in low power sleep mode. Understanding how to properly calibrate an end system when configuring these devices and possible sources of error is important.

Table of Contents

1 Introduction	2
2 AMR Angle Sensing	3
3 Calibrating AMR	4
3.1 Input Related Errors.....	4
3.2 Sensor Related Errors.....	6
3.3 Offset.....	7
3.4 Amplitude Mismatch.....	7
3.5 Orthogonality Error.....	7
3.6 Noise.....	7
4 Summary	8
5 References	8

Trademarks

All trademarks are the property of their respective owners.

1 Introduction

Unlike Hall-effect, Giant Magneto-Resistive (GMR), and Tunneling Magneto-Resistive elements (TMR), the Anisotropic Magneto-Resistive (AMR) sensing element does not have an output voltage proportional to the magnitude of the applied magnetic field in the direction of sensitivity. Rather, the AMR sensing element exhibits a change in resistance regarding the direction of the applied magnetic field vector.

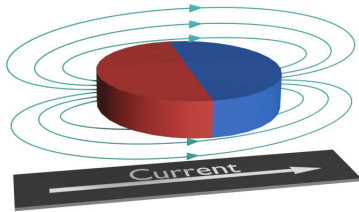


Figure 1-1. AMR Nominal Impedance Alignment

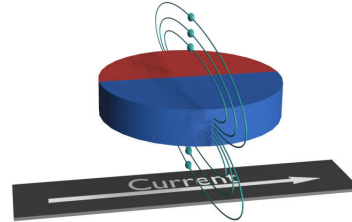


Figure 1-2. AMR Reduced Impedance Alignment

Figure 1-1 demonstrates that there is no resulting change in impedance with the magnetic field applied parallel to the flow of current through the sensing element. However, if the applied field is orthogonal to the sensing element then the impedance varies up to a maximal saturation point (Figure 1-2).

For example, suppose that the resistive element is exposed to an oscillating magnetic field, then the resulting behavior of the AMR resistivity follows the expression in Equation 1.

$$\rho(\theta) = \rho_{\parallel} + \rho_{\perp} \times (1 - \cos^2 \theta) \quad (1)$$

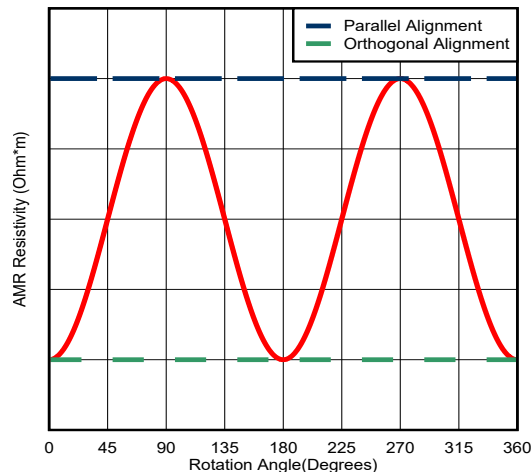


Figure 1-3. AMR Impedance vs Field Orientation

2 AMR Angle Sensing

The variation shown in [Figure 1-3](#) is particularly helpful if the sensor is setup in the format of a Wheatstone bridge, shown in [Figure 2-1](#). This particular configuration produces two parallel resistor dividers with elements physically orthogonal to each other. The variation in resistance results from the incident magnetic field producing a sinusoidal response as the field travels through a full rotation, balancing the structure with AMR elements with equally sized resistances along each axis.

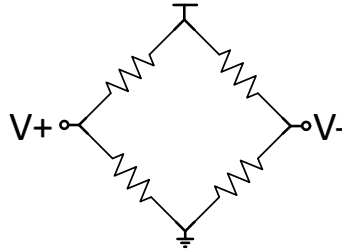


Figure 2-1. Wheatstone Bridge Configuration

What is particularly noteworthy about the response of the sensing element is that the output varies with $\cos^2\theta$. As a result, a typical AMR sensor produces two output cycles per revolution and a single Wheatstone bridge only directly resolves a physical rotation of 90° .

Given the response of the sensor to the rotating magnetic field, creating an electrically orthogonal set of sinusoidal outputs by integrating a second Wheatstone bridge rotated 45° is possible.

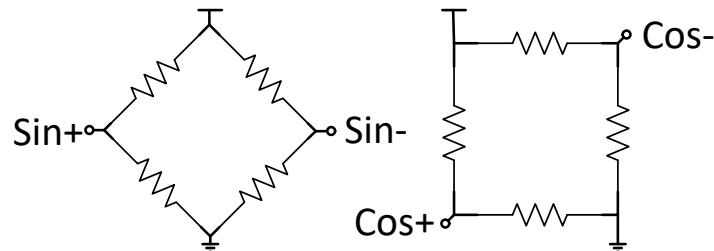


Figure 2-2. Sine and Cosine Wheatstone Arrangement

Together, the outputs represent sine and cosine, and can then be used to calculate an arctangent with a full 360° response for every 180° of mechanical rotation.

[TMAG6180-Q1](#) and [TMAG6181-Q1](#) take advantage of this sensing technology by combining a fast, two-dimension, Hall-effect latch to create an AMR sensor capable of detecting quadrant and extending the sensing range from 180° to the full 360° . [TMAG6180-Q1](#) generates Q0 and Q1 outputs which can calculate absolute angle. [TMAG6181-Q1](#) provides a turns counter that can increment or decrement at each quadrant change. This counter tracks the relative angle from power-on and absolute angle is possible if the turns counter is always initialized within the same 180° range.

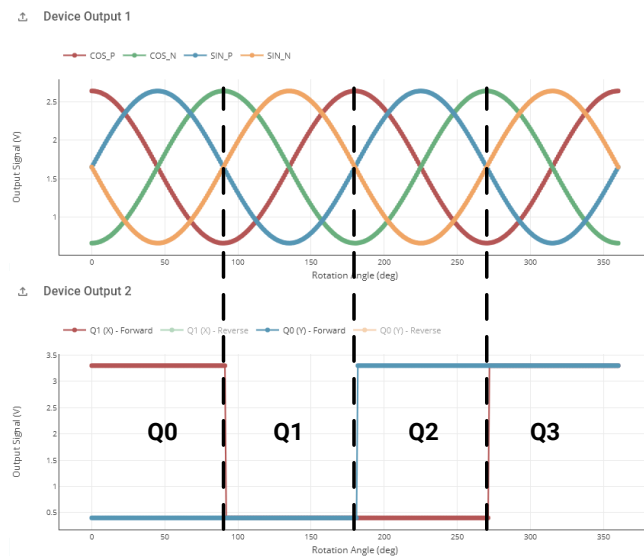


Figure 2-3. Simulated TMAG6180 Output Response

Automatic Gain Control (AGC) in both devices is set to produce outputs with a peak to peak amplitude of $0.6 \times V_{CC}$ with the output centered at $V_{CC}/2$, irrespective of the input magnetic field strength. The sensor adjusts the applied gain to maintain a constant output level following Equation 2 when changes in the magnetic field produce vector magnitude drift.

$$0.6 \times V_{CC} = \sqrt{\sin_{diff}^2 + \cos_{diff}^2} \tag{2}$$

The calculated signal typically swings between $\pm 0.6 \times V_{CC}$ when measured differentially. For example, when $V_{CC} = 3.3 \text{ V}$, each output signal can vary between 0.66 V and 2.64 V, and when taken differentially the resulting signal ranges between $\pm 1.98 \text{ V}$.

3 Calibrating AMR

3.1 Input Related Errors

AMR angle sensors are two dimensional in design but the complete magnetic field vector is 3D. The field vector parallels the face of the magnet when a magnet is centered on the axis of rotation along the pole boundary.

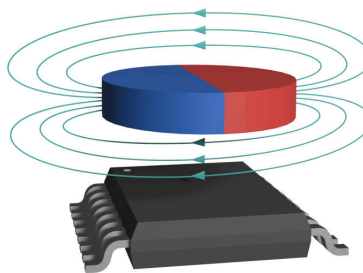


Figure 3-1. Correct Rotation Alignment

As a result, when the magnet rotates, the field vector is constrained in two dimensions and this produces the correct input for the sensor (Figure 3-1). The magnetic field vector varies in all three axes if the sensor is moved away from the axis of rotation.

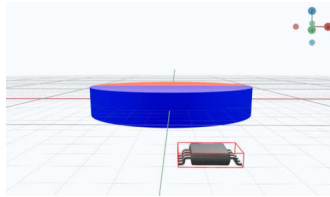


Figure 3-2. TMAG6180 With Mechanical Offset

The magnetic sensor is exposed to all three field components, with a circular profile presumption, but a significant portion of the input field in the z-direction is left undetected by the sensor. As a result, some input non-linearity is introduced. Consider the Lissajous plot in [Figure 3-3](#) that uses the full vector and projection onto the XY plane when the Z component is ignored in [Figure 3-4](#).

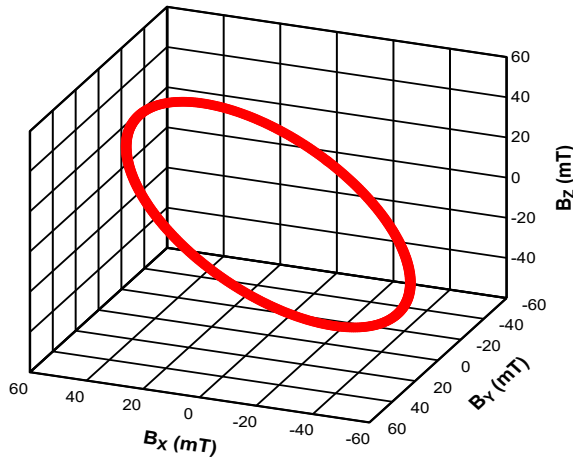


Figure 3-3. 3D Lissajous Plot

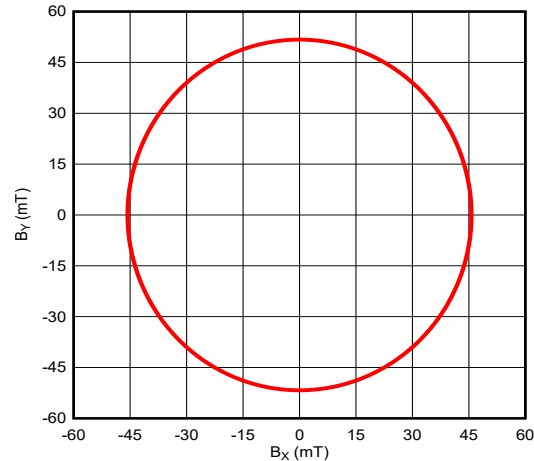


Figure 3-4. 2D Lissajous Projection

The resulting input magnetic field angle changes at a different rate than the mechanical rotation measured because the resulting projection is elliptical instead of circular (the extremes for the X direction are ± 45 mT while the Y direction is closer to 50 mT). The outputs generated by the device can take an unexpected form due to this non-linear change in angle. Careful examination of [Figure 3-5](#) reveals that the output waveforms are slightly distorted and not demonstrating correct sine and cosine behavior.

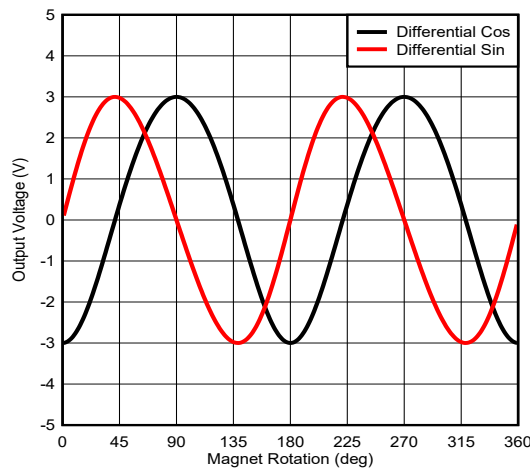


Figure 3-5. TMAG6180 Output Voltage with Mechanical Offset

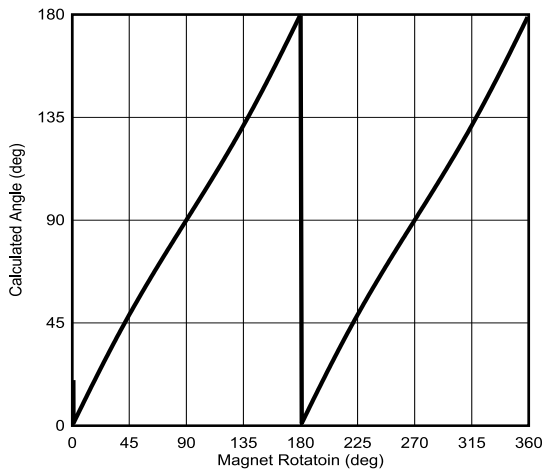


Figure 3-6. Calculated Angle With Mechanical Offset

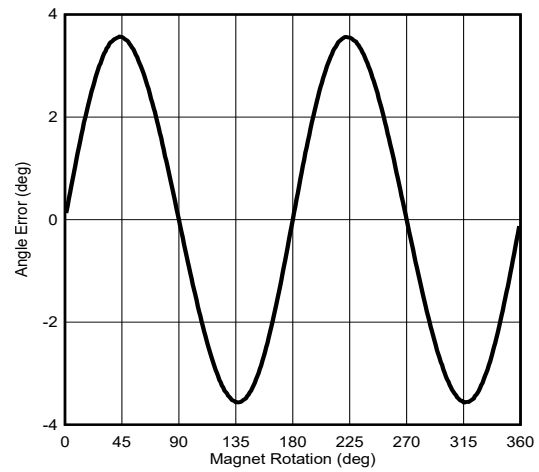


Figure 3-7. Angle Error Resulting From Mechanical Offset

The sensor outputs a non-linear angle calculation since the input to the sensor changes with a non-linear angle. This angle change is cyclical, so calibrating the sensor using techniques like multipoint linearization, a Look-up table, or harmonic approximation is available if necessary. These techniques are further described in [Achieving Highest System Angle Sensing Accuracy](#).

3.2 Sensor Related Errors

There are four main device-level sources of error to consider with any AMR angle sensor:

- Offset
- Amplitude Mismatch
- Orthogonality Error
- Noise

These errors are better understood by comparing multiple Lissajous curves against an error-free unit circle.

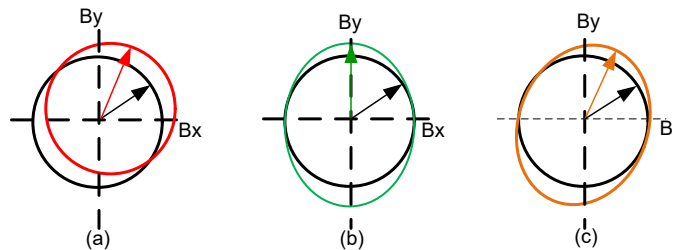


Figure 3-8. Angle Accuracy Impact Owing to Sensor Electrical Errors, Offset Error (a), Amplitude Mismatch Error (b), and Orthogonality Error (c)

Sections *Offset*, *Amplitude Mismatch*, and *Orthogonality Error* define the plot relationships of Figure 3-8. When differential outputs are available, the effective output mode can be described by Equation 3 and Equation 4. These relationships are used in subsequent calculations, but can be replaced with a single output if calculations are made with a single-ended value.

$$\sin_{\text{diff}} = \sin_p - \sin_N \tag{3}$$

$$\cos_{\text{diff}} = \cos_p - \cos_N \tag{4}$$

3.3 Offset

The Offset plot produces a circle that is not centered at the origin when either sine or cosine outputs are offset from the normal curve. This offset can be caused by an imbalance in the Wheatstone bridge or through a mismatch within the gain stage of the sensor.

After calculating the difference between the positive and negative outputs, any remaining offset is calculated and removed from either output signal by subtracting from the measured output differential (Equation 5 and Equation 6).

$$V_{os_sin} = \frac{\sin_{diff}(max) + \sin_{diff}(min)}{2} \quad (5)$$

$$V_{os_cos} = \frac{\cos_{diff}(max) + \cos_{diff}(min)}{2} \quad (6)$$

3.4 Amplitude Mismatch

Amplitude mismatch occurs with variations in channel sensitivity gain resulting in minor variations in the output amplitude of either the sine or cosine outputs. These variations skew the correct circular response shown in plot b of Figure 3-8.

The automatic gain control in TMAG6180-Q1 and TMAG6181-Q1 attempts to adjust channel sensitivity gain so the total magnitude is constant. However, some amount of mismatch can persist. Normalizing the two signals to the same amplitude removes this amplitude mismatch and minimizes this error source. This normalizing step occurs in post-processing using Equation 7 through Equation 9.

$$A_{sin_diff} = \frac{\sin_{diff}(max) - \sin_{diff}(min)}{2} \quad (7)$$

$$A_{cos_diff} = \frac{\cos_{diff}(max) - \cos_{diff}(min)}{2} \quad (8)$$

$$k = 1 - \left(\frac{A_{cos_diff}}{A_{sin_diff}} \right) \quad (9)$$

3.5 Orthogonality Error

Orthogonality error describes the effect of internal phase error between the sine and cosine outputs. These outputs at exactly 90 ° out of phase produces signals usable in an arctangent calculation. A non-linearity occurs if there is phase error in the outputs. This non-linearity requires more involved trigonometric transformations to correct. The error in phase is determined by comparing the zero crossing of the cosine output to the relative maximum of the sine output. Typically, this error is negligible for AMR sensors due to their construction. The method to remove a phase error, defined as β from an arctangent calculation, is shown in Equation 10.

$$\theta = \tan^{-1} \left(\frac{\cos(\beta)}{\left(\frac{\sin_{diff}}{\cos_{diff}} - \sin(\beta) \right)} \right) \quad (10)$$

3.6 Noise

Electrical noise is an unavoidable source of measurement error. The differential output of TMAG6180-Q1 and TMAG6181-Q1 help improve SNR. Understanding the impact on angle accuracy is important when considering SNR. Figure 3-9 shows how varying amounts of RMS output noise impacts the quality of an angle calculation. The error shown on each series assumes the maximum positive differential noise value, on the cosine output, with a maximum negative differential noise value, on the sine output. The resulting worst case angle error from noise is shown in Figure 3-9. The effective angle error remains fairly negligible in the case of an output referred noise of 0.5 mV RMS. However, an output filter, or oversampling, can be implemented to reduce noise further if desired.

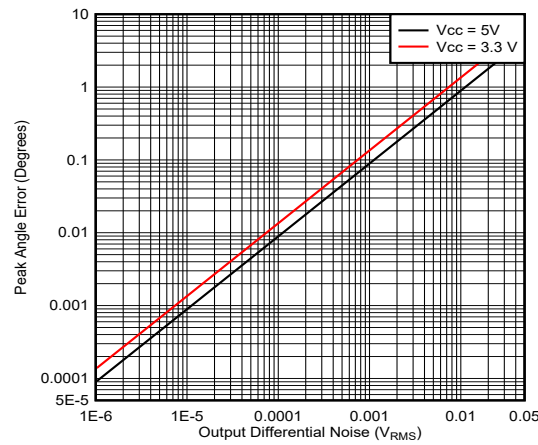


Figure 3-9. Angle Error Due to Worst-Case Peak to Peak Noise

4 Summary

AMR sensors provide benefits like reducing input noise and greatly improving response time when compared to traditional Hall-effect sensors. Creating non-linearity in the output response is possible by providing an input with non-linear angle change since these AMR sensors are designed to measure the angle of the input magnetic field vector in 2D space.

TI's [Magnetic Sense Simulator](#) (TIMSS) offers a convenient method to simulate magnetic fields and estimate device response. Using this tool allows users to create a rotating magnet and produce plots and data reports of the expected magnetic field and device response. These functions help users better understand what to expect before prototyping.

5 References

- Texas Instruments, [TMAG6180-Q1 Automotive High-Precision Analog AMR 360° Angle Sensor](#) data sheet
- Texas Instruments, [TMAG6181-Q1 High-Precision Analog AMR Angle Sensor With Integrated Turns Counter](#) data sheet
- Texas Instruments, [Achieving Highest System Angle Sensing Accuracy](#) application note
- Texas Instruments, [TI's Magnetic Sense Simulator](#) tool

IMPORTANT NOTICE AND DISCLAIMER

TI PROVIDES TECHNICAL AND RELIABILITY DATA (INCLUDING DATA SHEETS), DESIGN RESOURCES (INCLUDING REFERENCE DESIGNS), APPLICATION OR OTHER DESIGN ADVICE, WEB TOOLS, SAFETY INFORMATION, AND OTHER RESOURCES "AS IS" AND WITH ALL FAULTS, AND DISCLAIMS ALL WARRANTIES, EXPRESS AND IMPLIED, INCLUDING WITHOUT LIMITATION ANY IMPLIED WARRANTIES OF MERCHANTABILITY, FITNESS FOR A PARTICULAR PURPOSE OR NON-INFRINGEMENT OF THIRD PARTY INTELLECTUAL PROPERTY RIGHTS.

These resources are intended for skilled developers designing with TI products. You are solely responsible for (1) selecting the appropriate TI products for your application, (2) designing, validating and testing your application, and (3) ensuring your application meets applicable standards, and any other safety, security, regulatory or other requirements.

These resources are subject to change without notice. TI grants you permission to use these resources only for development of an application that uses the TI products described in the resource. Other reproduction and display of these resources is prohibited. No license is granted to any other TI intellectual property right or to any third party intellectual property right. TI disclaims responsibility for, and you will fully indemnify TI and its representatives against, any claims, damages, costs, losses, and liabilities arising out of your use of these resources.

TI's products are provided subject to [TI's Terms of Sale](#) or other applicable terms available either on [ti.com](https://www.ti.com) or provided in conjunction with such TI products. TI's provision of these resources does not expand or otherwise alter TI's applicable warranties or warranty disclaimers for TI products.

TI objects to and rejects any additional or different terms you may have proposed.

Mailing Address: Texas Instruments, Post Office Box 655303, Dallas, Texas 75265
Copyright © 2023, Texas Instruments Incorporated